Robotica (2018) volume 36, pp. 78–95. © Cambridge University Press 2017
doi:10.1017/S0263574717000169

Collision avoidance method for multi-operator multi-robot teleoperation system

S. E. García†*, E. Slawiñski†, V. Mut† and F. Penizzotto‡

†*Instituto de Automática, Universidad Nacional de San Juan, San Juan, Argentina.*
E-mails: sebasg@outlook.com, slawinski@inaut.unsj.edu.ar, vmut@inaut.unsj.edu.ar
‡*Instituto de Energía Eléctrica, Universidad Nacional de San Juan, San Juan, Argentina.*
E-mail: francopenizzotto@gmail.com

(Accepted March 11, 2017. First published online: April 3, 2017)

SUMMARY
This paper proposes a collision avoidance method for the teleoperation of multiple non-holonomic mobile robots from multiple users. Each human operator drives a mobile robot, where each one performs an independent task in a common workspace. To avoid collisions, the proposed method only acts on the speed of the mobile robots; therefore, the human operator can freely drive the robot over the path he chooses to. The developed analysis allows us to assure that a solution is always achieved. Finally, the results of the experiments are shown, in order to test the performance of the proposed control scheme.

KEYWORDS: Multi-operator; Multi-robot; Teleoperation system; Collision Avoidance; Mobile Robots.

1. Introduction

The teleoperation of mobile robots involves the operation of a remote vehicle at a distance, allowing the operator transport his ability to a remote environment, minimizing the associated dangers, or reaching places that are inaccessible for humans. In addition, recent works[1–3] have shown that robot-teleoperation systems can integrate complex automation methods and the human capacity in order to meet the task requirements. These systems are used in several applications, such as military/defensive, space, telesurgery, security, underwater vehicles, telerobotics in forestry and mining.[4] The teleoperation systems could be multi-operator and/or multi-robot types, allowing performing tasks in a cooperative manner or independent tasks performed simultaneously. Currently, the state of the art is diverse, in which different concepts and ideas are used. Several papers propose systems with a single human operator and multiple slave robots. For example, Fong *et al.*[5] propose and develop a collaborative control, with a dialogue in the form of questions, Suzuki *et al.*[6] propose a teleoperation system for inspection tasks, Lee *et al.*[7] and[8] present a control scheme for bilateral teleoperation, which ensure a secure and firm grip of an object and Rodriguez-Seda *et al.*[9] propose to control multiple aerial slave robots.

Moreover, few papers propose control schemes for multi-operator, multi-robot teleoperation systems. The following papers address this topic: in refs. [10]–[13], assisted control for remote collaboration in which two operators manipulate two robotic arms with collision probabilities is proposed; in refs. [14]–[16], a remote collaborative control with force reflection is proposed, where one operator manipulates a robotic arm, and another operator controls a mobile robotic arm, through internet; in refs. [17] and [18], collaborative teleoperation with force feedback is presented, where an object is gripped between two 1-DOF robots, which are manipulated by two operators.

On the other hand, in autonomous multiple mobile robotic systems, several methods for collision avoidance have been proposed. In ref. [19], a method of obstacle avoidance called Optimal Reciprocal Collision Avoidance (ORCA) is proposed. This proposal provides a sufficient condition for each

* Corresponding author. E-mail: sebasg@outlook.com

https://doi.org/10.1017/S0263574717000169 Published online by Cambridge University Press

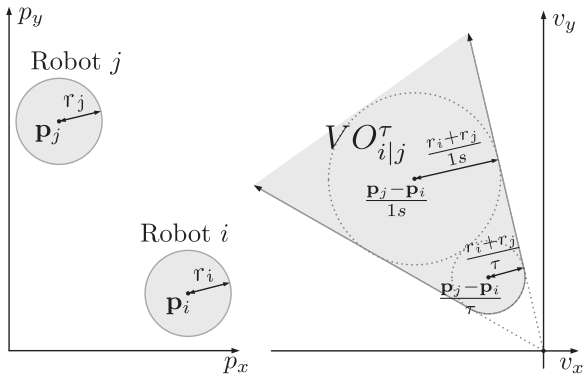


Fig. 1. Geometric interpretation of $VO^{\tau}_{i|j}$.

holonomic mobile robot to perform collision-free motions. Then, ref. [20] extends the ORCA method to non-holonomic mobile robots. This method is called NH-ORCA (ORCA under non-holonomic constraints). These 2D methods significantly modify the robots orientation; therefore, the use of these methods in teleoperation may not be suitable because these will change significantly the commands sent by the human operator, getting thus, a poor bilateral transparency.[21,22] Currently, these collision avoidance methods have been extended to aerial vehicles.[23–25]

This work proposes a multi-operator, multi-robot teleoperation system that includes a collision avoidance method.

Unlike the methods designed for autonomous robots, the proposed method only operates over the speed allowing the human operator a full control on the angular velocity at all times and therefore, the user can easily guide the robot through a desired path.

Besides, most of the methods designed for collision avoidance in multi-robot systems use optimization.

On the contrary, the proposed method always gets an approximated solution of low computational load, involving the search inside the linear velocity set (subset of the space formed by the linear and angular velocities), in each iteration in an explicit way.

The paper is organized as follows. First, the preliminaries are presented in Section 2. Then, in Section 3, the problem formulation is described. Section 4 presents the proposed collision avoidance method and Section 5 describes how the reference signals are obtained. A section about the implementation is showed in Section 6. Section 7 shows the obtained results. Discussion are presented in Section 8. The conclusion is given in Section 9. Finally, two appendixes are included.

2. Preliminaries

Also, in ref [26], a concept known as velocity obstacle, which considers disk-shape obstacles, is defined. These proposal is redefined in ref. [19] as follows.

For two robots, assuming that the robots have a disk shape with radius r_i and they move in the $\mathbb{R}^2$ plane with current position $\mathbf{p}_i$ and current velocity $\mathbf{v}_i$, the velocity obstacle set for robot i induced by another robot j,$(j \neq i)$ is defined as the set of all relative velocities $\mathbf{v_r} = \mathbf{v}_i - \mathbf{v}_j$ that will result in a collision between robots i and j before a preset time τ:

$$VO^{\tau}_{i|j} = \left\{\mathbf{v_r} : \exists t \in [0, \tau] \,|\, t\mathbf{v_r} \in B\left(\mathbf{p}_j - \mathbf{p}_i, r_i + r_j\right)\right\} \tag{1}$$

with $B(\mathbf{p}, r) = \{\mathbf{q} \in \mathbb{R}^2 \mid \|\mathbf{q} - \mathbf{p}\| \leq r\}$, which is the closed ball of radius r centered at $\mathbf{p}$. The sets $VO^{\tau}_{i|j}$ and $VO^{\tau}_{j|i}$ are symmetric in reference to the origin. Figure 1 shows the geometric interpretation of the velocity obstacle set $VO^{\tau}_{i|j}$, where $v_x = \partial p_x/\partial t$ and $v_y = \partial p_y/\partial t$. Also, $VO^{\infty}_{i|j}$ is defined as follows:

$$VO^{\infty}_{i|j} = \lim_{\tau \to \infty} VO^{\tau}_{i|j} = \left\{\mathbf{v_r} : \exists t \in [0, \infty) \,|\, t\mathbf{v_r} \in B\left(\mathbf{p}_j - \mathbf{p}_i, r_i + r_j\right)\right\} \tag{2}$$

https://doi.org/10.1017/S0263574717000169 Published online by Cambridge University Press

Now the open set for collision avoidance is defined as the set of the all relative velocities $\mathbf{v}_{i|j} = \mathbf{v}_i - \mathbf{v}_j$ that guarantee free collisions movements, i.e., the complement of the set $VO^{\tau}_{i|j}$:

$$CA^{\tau}_{i|j} = \left\{\mathbf{v_r} | \mathbf{v_r} \notin VO^{\tau}_{i|j}\right\} \tag{3}$$

3. Problem Formulation

This work addresses a teleoperation system with $n \in \mathbb{N}$ human operators, each one teleoperating one of n non-holonomic mobile robots under a shared environment. These systems have several applications in safety. For example, a risky situation where different operators handle firefighter robots (teleoperated) to rescue humans, in a forest fire. The vision of operators could be interrupted by smoke, generating a high probability of collision.

It is assumed that the robots have a disk shape with radius $r_i \in \mathbb{R}$, moving them in the $\mathbb{R}^2$ space with current position $\mathbf{p}_i \in \mathbb{R}^2$, speed $\upsilon_i \in \mathbb{R}$, angular velocity $\omega_i \in \mathbb{R}$ and velocity vector $\mathbf{v}_i \in \mathbb{R}^2$ according to υ_i and the robot's orientation. Each human operator generates linear and angular velocity references, $\upsilon_i^{Href} \in \mathbb{R}$ and $\omega_i^{Href} \in \mathbb{R}$, respectively, using a hand controller device. In addition, the control actions of the robots are the speed $\upsilon_i^{Rref} \in \mathbb{R}$ and angular velocity $\omega_i^{Rref} \in \mathbb{R}$.

In order to avoid collisions, the velocity of the robot is modified. However, a change on the angular velocity is invasive to the human, causing the loss of transparency.[22] If the robots speed increases or changes its sense, or if the robot changes its orientation; then the human operator could be confused. Instead, a decrease of the robots' speed involves an energy dissipation that commonly is a change that does not generates risk nor a confusing state. Therefore, a collision avoidance method is proposed, which does not increase the robots' speed, does not modify its sense of advance and does not changes the robots orientation.

To achieve that, the following design guidelines are proposed: $|\upsilon_i^{Rref}| \leq |\upsilon_i^{Href}|$, and υ_i^{Rref} as close as possible to υ_i^{Href}. A collision avoidance method is proposed to obtain the reference of speed υ_i^{Rref} for the robot that ensures collision-free movements.

In this way, the angular velocity is always controlled by the human operator (i.e., $\omega_i^{Rref} = \omega_i^{Href}$), getting thus a high level of control of the robot.

It is important to point out that for each robot the collision avoidance method requires information from other robots, and the velocity references generated by the human operator (Fig. 2).

4. Speed Collision Avoidance (SCA)

Considering two robots i and j, to avoid collision, the vector of relative velocity $\mathbf{v}_i - \mathbf{v}_j$ must lay outside $VO^{\tau}_{i|j}$. Thus, for each robot i, a set of permitted speeds called $SCA^{\tau}_{i|j}$ that ensure $\mathbf{v}_i - \mathbf{v}_j \notin VO^{\tau}_{i|j}$ will be obtained:

$$SCA^{\tau}_{i|j} = \left\{\upsilon | \upsilon \in \left[0, \upsilon^{\lim}_{i|j}\right)\right\} \tag{4}$$

where $\upsilon^{\lim}_{i|j}$ is an upper limit of speed of robot i. Any value of speed υ_i less than $\upsilon^{\lim}_{i|j}$ avoids the collision with robot j.

The intersection of all $SCA^{\tau}_{i|j}$ for $j \neq i$ will give as result the set SCA^{τ}_i of permitted speed that robot i can take to guarantee collision avoidance:

$$SCA^{\tau}_i = \bigcap_{j \neq i} SCA^{\tau}_{i|j} = \left\{\upsilon | \upsilon \in \left[0, \upsilon^{\lim}_i\right)\right\} \tag{5}$$

where $\upsilon^{\lim}_i = \min_{j \neq i}\left(\upsilon^{\lim}_{i|j}\right)$.

Four possible situations between pairs of robots could happen. The first situation occurs when $\mathbf{v}_i \notin VO^{\infty}_{i|j}$ and $\mathbf{v}_j \notin VO^{\infty}_{j|i}$. This situation is denominated out–out. The in–out situation happens when $\mathbf{v}_i \in VO^{\infty}_{i|j}$ and $\mathbf{v}_j \notin VO^{\infty}_{j|i}$. The opposite situation to the last one is called out–in, where $\mathbf{v}_i \notin VO^{\infty}_{i|j}$

https://doi.org/10.1017/S0263574717000169 Published online by Cambridge University Press

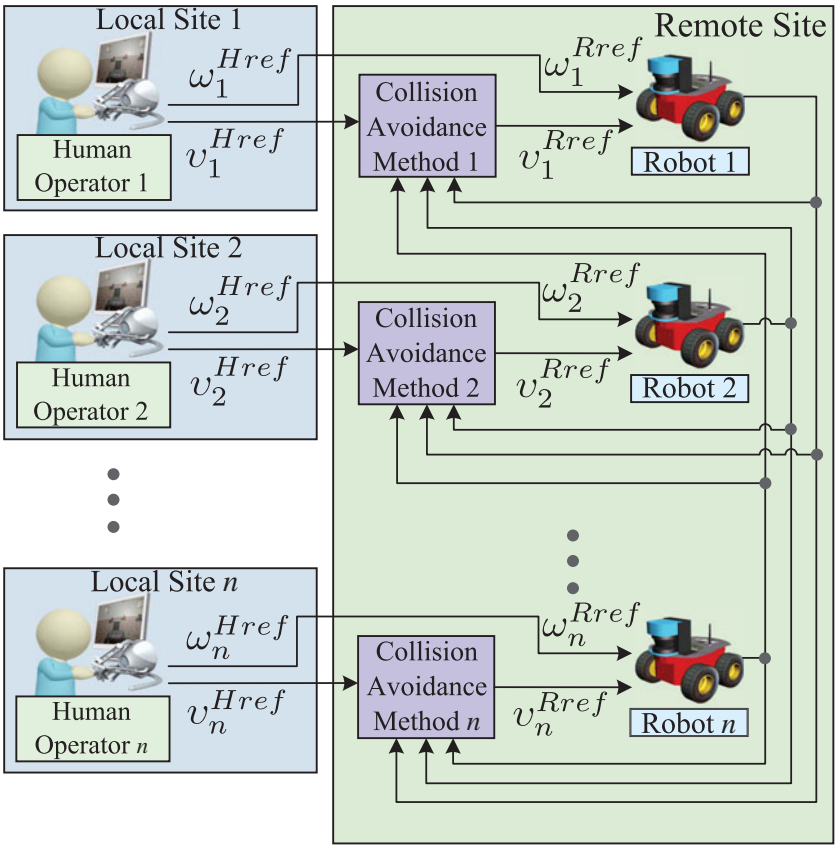


Fig. 2. Teleoperation system with n users and n robots.

and $\mathbf{v}_j \in VO^{\infty}_{j|i}$. The last possible situation is called in–in, where $\mathbf{v}_i \in VO^{\infty}_{i|j}$ and $\mathbf{v}_j \in VO^{\infty}_{j|i}$. These situations are described and analyzed in the next four subsections.

4.1. Out–out situation

In this situation, neither of the two robots moves toward the other; therefore, $\mathbf{v}_i \notin VO^{\infty}_{i|j}$ and $\mathbf{v}_j \notin VO^{\infty}_{j|i}$. As $\mathbf{v}_j \notin VO^{\infty}_{j|i}$, $-\mathbf{v}_j \notin VO^{\tau}_{i|j}$, because $VO^{\tau}_{i|j}$ and $VO^{\tau}_{j|i}$ are symmetric in reference to the origin, and $VO^{\tau}_{i|j} \subset VO^{\infty}_{i|j}$. We consider one of the two robots as an obstacle and the other will be the responsible for avoiding the collision. Here, it is necessary to define a criterion to select the robot that will be considered as an obstacle. For example, a criterion could be the selection of the robot that is coming from the right, or chose the one that has a higher speed. In this paper, the second criterion is used.

Figure 3 shows two out–out situations. In the first situation (Fig. 3(a)), robot i has a speed that is lower than the one of robot j, which is considered as an obstacle. The new velocity vector of robot i is set to $\lambda_i \mathbf{v}_i$, with $\lambda_i > 0$. The objective is to obtain an upper bound $\lambda_i^{\lim}(t)$ of λ_i, where $\lambda_i^{\lim}(t)\mathbf{v}_i - \mathbf{v}_j$ belongs to the boundary of $VO^{\tau}_{i|j}$ ($\partial VO^{\tau}_{i|j}$), as it is shown in Fig. 3(a). If $0 < \lambda_i < \lambda_i^{\lim}(t)$, then collision-free movement will be guaranteed ($\lambda_i \mathbf{v}_i - \mathbf{v}_j \notin VO^{\tau}_{i|j}$). Then, the value of $\upsilon^{\lim}_{i|j}$ from the set $SCA^{\tau}_{i|j}$ is getting as $\upsilon^{\lim}_{i|j} = \lambda_i^{\lim}(t)\upsilon_i$.

Lemma 1. *If* $\mathbf{v}_\beta \notin VO^{\tau}_{i|j}$ *and* $\mathbf{v}_\alpha \in R^2$, *then there are values of* $\lambda > 0$ *such that* $\lambda\mathbf{v}_\alpha + \mathbf{v}_\beta \notin VO^{\tau}_{i|j}$.

See Appendix A for the corresponding proof of *Lemma 1*. Now, taking in *Lemma 1* $\mathbf{v}_\beta = -\mathbf{v}_j$ and $\mathbf{v}_\alpha = \mathbf{v}_i$, and then there are values of $\lambda_i > 0$ such that $\lambda_i \mathbf{v}_i - \mathbf{v}_j \notin VO^{\tau}_{i|j}$.

The value $\lambda_i^{\lim}(t)$ can be obtained geometrically for each time instant intersecting the line segment:

$$\mathbf{v}_{i|j}(\lambda_i) = \lambda_i \mathbf{v}_i - \mathbf{v}_j \quad \lambda_i > 0 \tag{6}$$

https://doi.org/10.1017/S0263574717000169 Published online by Cambridge University Press

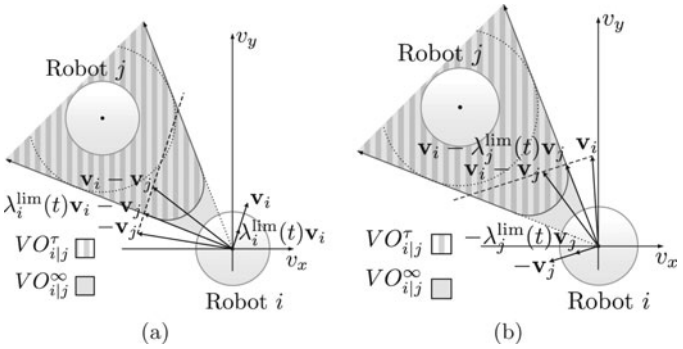


Fig. 3. Out-out situations.

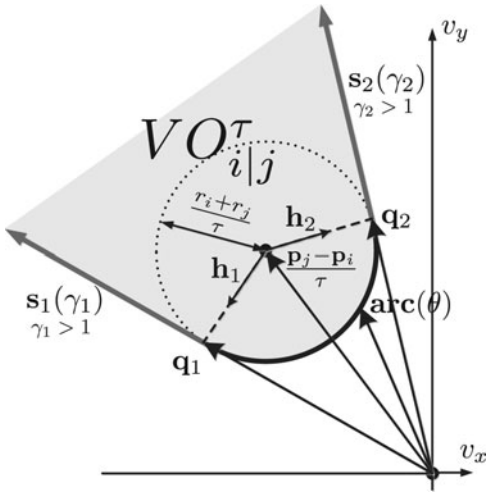


Fig. 4. Velocity obstacle set and vectors $\mathbf{q}_1$, $\mathbf{q}_2$, $\mathbf{s}_1(\gamma_1)$, $\mathbf{s}_2(\gamma_2)$, and $\mathbf{arc}(\theta)$.

with the boundary of $VOij$ ($\partial VO^{\tau}_{i|j}$), which can be broken down in two line segments and a circular arc.

The line segments of $\partial VO^{\tau}_{i|j}$ (see Fig. 4) are given by

$$\mathbf{s}_l(\gamma_l) = \gamma_l \mathbf{q}_l \quad \gamma_l > 1 \quad \text{for } l = 1,\ 2 \tag{7}$$

with

$$\mathbf{q}_1 = \left(\mathbf{I} - \frac{(r_i + r_j)\left((r_i + r_j)\mathbf{I} - \mu\mathbf{R}\right)}{\|\mathbf{p}_j - \mathbf{p}_i\|^2}\right)\frac{(\mathbf{p}_j - \mathbf{p}_i)}{\tau} \tag{8a}$$

$$\mathbf{q}_2 = \left(\mathbf{I} - \frac{(r_i + r_j)\left((r_i + r_j)\mathbf{I} + \mu\mathbf{R}\right)}{\|\mathbf{p}_j - \mathbf{p}_i\|^2}\right)\frac{(\mathbf{p}_j - \mathbf{p}_i)}{\tau} \tag{8b}$$

where $\mu = \sqrt{\|\mathbf{p}_j - \mathbf{p}_i\|^2 - (r_i + r_j)^2}$ and $\mathbf{R} = \left[\begin{smallmatrix} 0 & -1 \\ 1 & 0 \end{smallmatrix}\right]$.

The deduction of the vectors $\mathbf{q}_1$ and $\mathbf{q}_2$ is shown in Appendix B.

On the other hand, the circular arc is given by

$$\mathbf{arc}(\theta) = \frac{(\mathbf{p}_j - \mathbf{p}_i)}{\tau} + \frac{(r_i + r_j)}{\tau}[\cos(\theta)\ \sin(\theta)]^T \tag{9}$$
$$\text{for } \theta_1 < \theta < \theta_2$$

https://doi.org/10.1017/S0263574717000169 Published online by Cambridge University Press

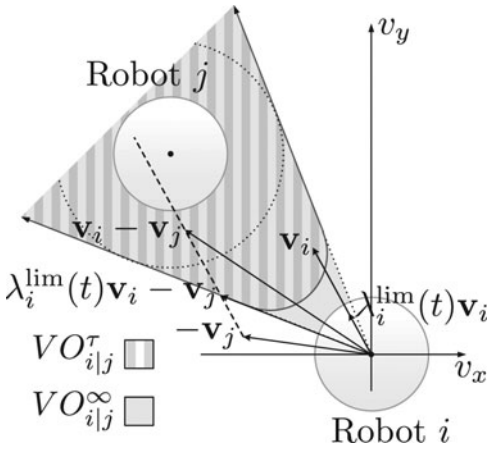


Fig. 5. In–out situation.

where

$$\theta_l = \arctan\left(\frac{\left(\mathbf{q}_l - \left(\mathbf{p}_j - \mathbf{p}_i\right)/\tau\right)^T [0\ \ 1]^T}{\left(\mathbf{q}_l - \left(\mathbf{p}_j - \mathbf{p}_i\right)/\tau\right)^T [1\ \ 0]^T}\right) \tag{10}$$

The intersection between (6) and (7) results (see Appendix B):

$$\lambda_{i_l} = \frac{\mathbf{v}_j^T \mathbf{R}\mathbf{q}_l}{\mathbf{v}_i^T \mathbf{R}\mathbf{q}_l} \quad \text{for } l = 1,\ 2 \tag{11a}$$

$$\gamma_l = \frac{\mathbf{v}_j^T \mathbf{R}\mathbf{v}_i}{\mathbf{v}_i^T \mathbf{R}\mathbf{q}_l} \quad \text{for } l = 1,\ 2 \tag{11b}$$

Now, if $\lambda_{i_l} > 0$ and $\gamma_l > 1$, for $l = 1,\ 2$, then the corresponding line segments are intersected.
The intersection between (6) and (9) gives as result (see Appendix B):

$$\lambda_{i_3} = \frac{\mathbf{v}_i^T \left(\frac{\mathbf{p}_j - \mathbf{p}_i}{\tau} + \mathbf{v}_j\right)}{\|\mathbf{v}_i\|^2} - \frac{\sqrt{\|\mathbf{v}_i\|^2 \left(\frac{r_i + r_j}{\tau}\right)^2 - \left(\mathbf{v}_i^T \mathbf{R}\left(\frac{\mathbf{p}_j - \mathbf{p}_i}{\tau} + \mathbf{v}_j\right)\right)^2}}{\|\mathbf{v}_i\|^2} \tag{12}$$

If λ_{i_3} is real and greater than zero, then $\mathbf{v}_{i|j}(\lambda_i)$ and $\mathbf{arc}(\theta)$ are intersected.
Because many intersections could occur, $\lambda_i^{\lim}(t)$ is taken as follows:

$$\lambda_i^{\lim}(t) = \min\left(\lambda_{i_l}\right) \tag{13}$$

where only λ_{i_l} corresponding to valid intersections are considered.

In the second situation (Fig. 3(b)), robot i has a speed that is higher than the one of robot j; therefore, robot i is considered as an obstacle. Thus, robot i may take any value of speed. Then, $\upsilon_{i|j}^{\lim} = \upsilon_i^{\max}$, where $\upsilon_i^{\max}$ is the maximal speed of robot i.

4.2. In–out situation

In this situation, robot i moves towards robot j (Fig. 5). For this reason, robot i should be responsible for avoiding the collision, and therefore, robot j is considered as an obstacle.

The value of $\upsilon_{i|j}^{\lim} = \lambda_i^{\lim}(t)\upsilon_i$, where $\lambda_i^{\lim}(t)$ is obtained like in Section 4.1.

Lemma 1 is also valid for this situation, which means that $\lambda_i^{\lim}(t)$ will be always positive.

https://doi.org/10.1017/S0263574717000169 Published online by Cambridge University Press

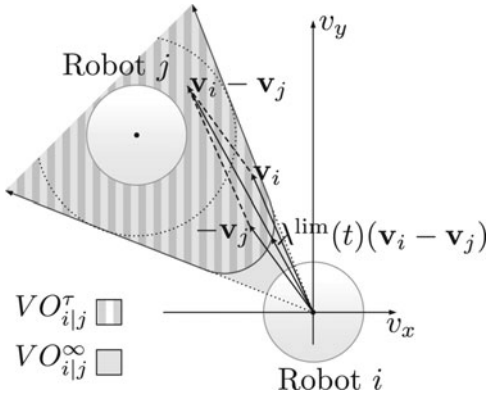


Fig. 6. In–in situation.

4.3. Out–in situation

This situation is opposite to the one explained immediately above, where $\mathbf{v}_i \notin VO^{\infty}_{i|j}$ and $\mathbf{v}_j \in VO^{\infty}_{j|i}$. Thus, robot i is considered as an obstacle. Therefore, robot i may take the speed generated by the human operator at all times, and therefore, $\upsilon^{\lim}_{i|j} = \upsilon^{\max}_i$.

4.4. In–in situation

This situation occurs when both robots go towards the other, thus $\mathbf{v}_i \in VO^{\infty}_{i|j}$ and $\mathbf{v}_j \in VO^{\infty}_{j|i}$. Figure 6 shows this situation. Here, neither of the two robots can be considered as an obstacle, and therefore upper bounds $\lambda^{\lim}_i(t)$ and $\lambda^{\lim}_j(t)$ for both robots must be obtained.

Lemma 2. *If* $\mathbf{v}_i \in VO^{\infty}_{i|j}$ *and* $-\mathbf{v}_j \in VO^{\infty}_{i|j}$, *then* $\lambda_i\mathbf{v}_i - \lambda_j\mathbf{v}_j \in VO^{\infty}_{i|j}$ *for* $\lambda_i > 0$ *and* $\lambda_j > 0$.

The *Lemma 2* is proven in Appendix A. *Lemma 2* shows that if the human operators do not change the direction of the robots, these will remain in the in–in situation.

To avoid a collision in this situation, it is necessary to find bounds $\lambda^{\lim}_i(t)$ and $\lambda^{\lim}_j(t)$ of λ_i and λ_j, respectively ($\lambda_i < \lambda^{\lim}_i(t)$ and $\lambda_j < \lambda^{\lim}_j(t)$) to ensure that $\lambda^{\lim}_i(t)\mathbf{v}_i - \lambda^{\lim}_j(t)\mathbf{v}_j \in \partial VO^{\tau}_{i|j}$.

We reduce the search to 1 degree of freedom in order to find a unique solution, proposing $\lambda^{\lim}_i(t) = \lambda^{\lim}_j(t) = \lambda^{\lim}(t)$. So if $\mathbf{v}_i - \mathbf{v}_j \in VO^{\tau}_{i|j}$, a reduction of the speed in the same proportion for both robots is caused. Thus, the new problem is to find the value $\lambda^{\lim}(t) > 0$ to ensure that $\lambda^{\lim}(t)(\mathbf{v}_i - \mathbf{v}_j) \in \partial VO^{\tau}_{i|j}$. Since the null vector ($\mathbf{0}$) does not belong to $VO^{\tau}_{i|j}$, and taking in *Lemma 1* $\mathbf{v}_\beta = \mathbf{0}$ and $\mathbf{v}_\alpha = \mathbf{v}_i - \mathbf{v}_j$, there exists $\lambda > 0$ such that $\lambda(\mathbf{v}_i - \mathbf{v}_j) \notin VO^{\tau}_{i|j}$.

The upper bound $\lambda^{\lim}(t)$ can be obtained geometrically intersecting the line segment:

$$\mathbf{v}_{i|j}(\lambda) = \lambda\left(\mathbf{v}_i - \mathbf{v}_j\right) \quad \text{for } \lambda > 0 \tag{14}$$

with the circular arc of $\partial VO^{\tau}_{i|j}$ given by (9), which gives

$$\lambda^{\lim}(t) = \frac{\left(\mathbf{v}_i - \mathbf{v}_j\right)^T\left(\frac{\mathbf{p}_j - \mathbf{p}_i}{\tau}\right)}{\left\|\mathbf{v}_i - \mathbf{v}_j\right\|^2} - \frac{\sqrt{\left\|\mathbf{v}_i - \mathbf{v}_j\right\|^2\left(\frac{r_i + r_j}{\tau}\right)^2 - \left(\left(\mathbf{v}_i - \mathbf{v}_j\right)^T\mathbf{R}\left(\frac{\mathbf{p}_j - \mathbf{p}_i}{\tau}\right)\right)^2}}{\left\|\mathbf{v}_i - \mathbf{v}_j\right\|^2} \tag{15}$$

The result given by (15) was obtained in a way similar to the procedure followed to get (12).

Then, $\upsilon^{\lim}_{i|j} = \lambda^{\lim}_i(t)\upsilon_i$.

The proposed collision avoidance method modifies the velocity vector magnitude; therefore, it can be applied to non-holonomic as well as holonomic mobile robots.

4.5. Robots with zero speed

The proposed method works with vectors. For each robot with speed slower than a defined value ε near to 0, a vector with magnitude ε and direction according to the current orientation is defined.

https://doi.org/10.1017/S0263574717000169 Published online by Cambridge University Press

This vector is used in order to obtain $\upsilon_{i|j}^{\lim}$. If the robot is holonomic, then it is necessary to get $\upsilon_{i|j}^{\lim}$ considering the orientation that will generate the lower $\upsilon_{i|j}^{\lim}$.

4.6. Steps of the algorithm

For robot i, the method consists in the following points:

(1) Determine the situation type.
(2) Get the set $SCA_{i|j}^{\tau}$ for each robot i different of robot j.
(3) Get the set $SCA_i^{\tau} = \bigcap_{j \neq i} SCA_{i|j}^{\tau}$.
(4) Get the reference of speed for the robot that guarantees collision-free movements:

$$\upsilon_i^{Rref} = \begin{cases} \upsilon_i & \text{if } \upsilon_i < \upsilon_i^{\lim} \\ \upsilon_i^{\lim} - \rho & \text{if } \upsilon_i \geq \upsilon_i^{\lim} \end{cases} \tag{16}$$

where $0 < \rho < \upsilon_i^{\max}$ is a adjustment parameter that ensures that at each iteration the speed decreases by at least ρ when robot i has speed that would cause a collision (that is $\upsilon_i \geq \upsilon_i^{\lim}$). If $(\upsilon_i^{\lim} - \rho) < 0$, then $\upsilon_i^{Rref} = 0$.

(5) Repeat steps 1 to 4 until $\upsilon_i < \upsilon_i^{\lim}$ for all the robots (for $i = 1, \ldots, n$). If $\upsilon_i^{\lim}$ in the iteration k is greater than the one computed in the previous iteration $k-1$, then $\upsilon_i^{\lim}$ in k is replaced by $\upsilon_i^{\lim}$ of $k-1$, where $k \in \mathbb{N}$.

In each iteration at least one robot decreases its speed by ρ, as minimum. Although it is not common in practice, a valid theoretical solution is to get a null speed for all robots. In this case, the teleoperators can change their angular velocity commands to get out from this situation, since such commands are not modified by the proposed algorithm. Then, in the worst-case scenario, the maximum number of possible iterations is

$$I^{max} = n \left\lceil \frac{\upsilon_i^{\max}}{\rho} \right\rceil \tag{17}$$

The choice of the value of ρ is a trade-off between convergence speed of the algorithm and a solution closer to the optimal. The smaller the ρ, the greater the I^{max} and the smaller the $(\upsilon_i - \upsilon_i^{Rref})$.

5. Master Devices Used

The human operator generates speed reference υ_i^{Href} and angular velocity reference ω_i^{Href} using a joystick or steering wheel. The proposal method is independent of the device that is used. The devices used in this paper were one Logitech G27 Steering Wheel, two Novint Falcon 3D Joystick and one Logitech Attack 3 Joystick (Fig. 7).

The mapping of the coordinates of the used devices to velocity commands is performed as follows:

$$\begin{bmatrix} \upsilon_i^{Href} \\ \omega_i^{Href} \end{bmatrix} = \begin{bmatrix} k_{g_{\upsilon_i}} q_{m_x} \\ k_{g_{\omega_i}} q_{m_y} \end{bmatrix} \tag{18a}$$

or

$$\begin{bmatrix} \upsilon_i^{Href} \\ \omega_i^{Href} \end{bmatrix} = \begin{bmatrix} k_{g_{\upsilon_i}} (a-b)\cos(\theta) \\ k_{g_{\omega_i}} (a-b)\sin(\theta) \end{bmatrix} \tag{18b}$$

where q_{m_x} and q_{m_y} correspond to the cartesian coordinates in plane x–y of the position vector $\mathbf{q_m} \in \mathbb{R}^2$ for the Logitech Attack 3 Joystick, and the position vector $\mathbf{q_m} \in \mathbb{R}^3$ for the Novint Falcon 3D Joystick ($q_{m_z} = 0$). The signals a, b, and θ represent the accelerator pedal position, brake pedal position, and angular position of steering wheel ($-90^\circ < \theta < 90^\circ$), respectively. $k_{g_{\upsilon_i}}$ and $k_{g_{\omega_i}}$ are gain parameters that scale the position of the master device to velocity commands.

https://doi.org/10.1017/S0263574717000169 Published online by Cambridge University Press

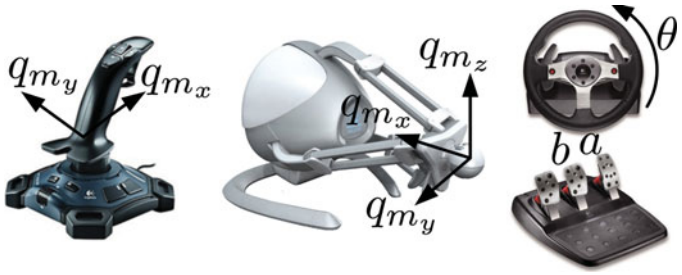


Fig. 7. Logitech Attack 3 Joystick, Novint Falcon 3D Joystick, and Logitech G27 Steering Wheel.

6. Implementation

To test the performance of the system, a software architecture for systems composed of multiples non-holonomic mobile robots and multiples users connected by a computer network was developed.

The software architecture is based on a platform of multiples servers associated with the robots as well as multiples clients associated with the users, all linked through the central application. The block diagram of Fig. 9 shows the different applications that integrate the software system.

These applications are called Central, Robot, Human, and Joystick application. The Central app receives the following information: the states of each non-holonomic mobile robot from each Robot server, and the references generated by each user through the Human client. In Central app, the control actions for each robot are processed. The communication between the Central, Human and Robot applications is carried out via UDP, allowing that these apps can run on different computers. The Human app acts as intermediary between the Central and the Joystick Application, sending to the Central the reference generated by the human operator. Using shared memory, the Human exchanged data with the Joystick application. In this way, it is easy to integrate any new hand controller in the system.

On the other hand, for the transmission of video, webcams and android-phones on the robots were used. We used server applications for cameras. For the web-cams, the yawcam app (http://www.yawcam.com) was used. Also, the ipwebcam app, which can be downloaded from google play (https://play.google.com), was used for the android phones. Each human operator visualized the camera image through a web browser, in the local site.

7. Experimental Tests

In this section, the collision avoidance method for the proposed teleoperation system is tested. As robots have dynamic, a virtual radius bigger than the radius of the circle that cover the robot was considered for safety. Robots are covered by a circle of radius of 0.3 m. The maximal speed set for the robot was $\upsilon_i^{\max} = 0.5$. Two tests were performed in which a virtual radius $r_i = 0.5$ m, a time horizon $\tau = 3s$, and $\rho = 0.05$ m/s were set. Also, the maximum commands of linear and angular velocities are $0.5\frac{m}{s}$ and $0.5\frac{rad}{s}$, respectively.

7.1. First test

In a common environment, four non-holonomic mobile robots (two Pioneer 3AT, one Pioneer 3DX, and one Pioneer 2) are teleoperated by four human operators (see Fig. 8). The operators 1 and 3 used Novint Falcon 3D joysticks. The operators 2 and 4 used the Logitech Attack 3 Joystick and the Logitech G27 Steering Wheel. The task, for each human operator, consists in moving one robot from a corner to the opposite one. Robots 1, 2, 3 and 4 begin in positions $[2.5\ 2.5]^T$, $[-2.5\ 2.5]^T$, $[-2.5\ -2.5]^T$ and $[2.5\ -2.5]^T$. The goal is that the robots go to $[-2.5\ -2.5]^T$, $[2.5\ -2.5]^T$, $[2.5\ 2.5]^T$ and $[-2.5\ 2.5]^T$. These positions are in meters.

Figure 10 shows the speed command generated by the user, the speed given by the proposed algorithm and the robots current speed (top subplot). Also, on the middle subplot, the angular velocity command given by the user and the robots angular velocity is showed. And, the different situations of the robot 2 respect to the other robots are showed in the bottom subplot, where o–o, i–o, o–i and i–i are the out–out, in–out, out–in and in–in situations, respectively. All signals correspond

https://doi.org/10.1017/S0263574717000169 Published online by Cambridge University Press

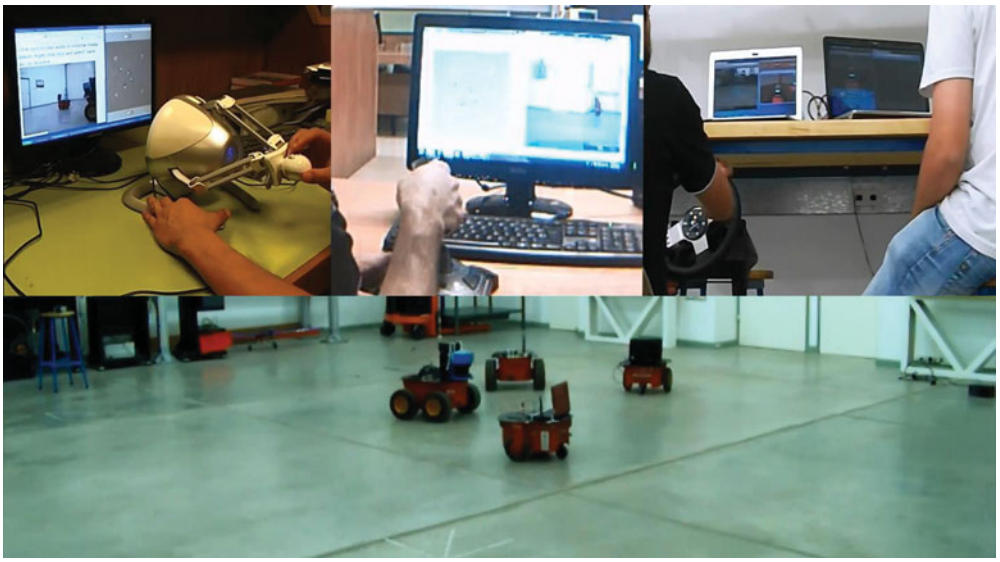


Fig. 8. Human operators in the local sites and mobile robots in the remote site.

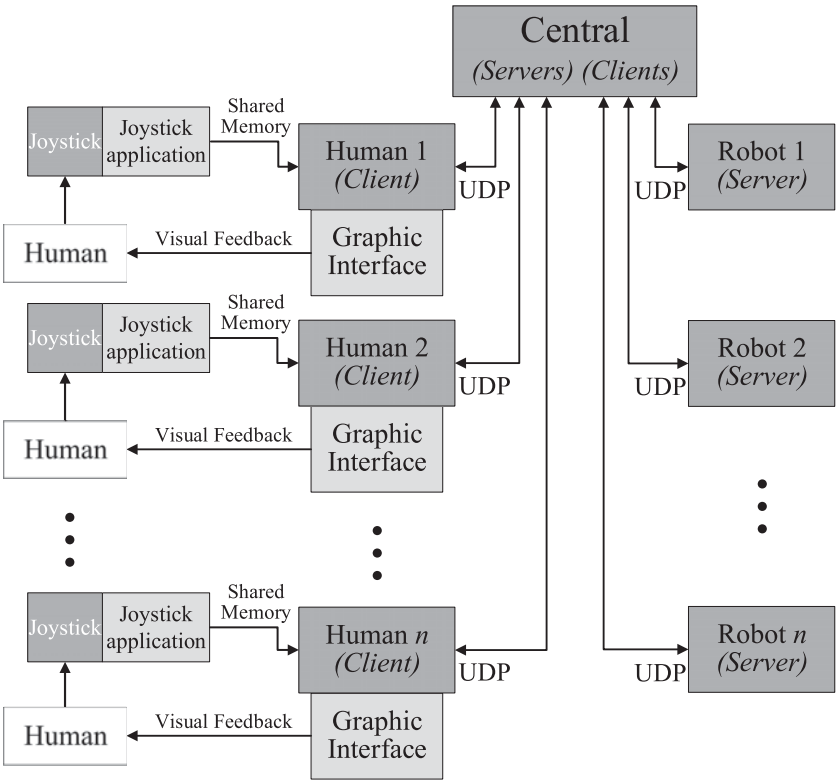


Fig. 9. Block diagram of software architecture.

to robot 2. It is observed that the robots current velocities are affected by the robots dynamics. If the robots dynamics is slower, a larger virtual radius r_i and/or a larger time horizon τ should be considered, for safety.

On the other hand, it is possible to appreciate that the proposed guidelines are fulfilled in practice, for example $|\upsilon_i^{Rref}| \leq |\upsilon_i^{Href}|$ for all time.

The trajectories performing for each of the robots are shown in Fig. 11. Each trajectory is color coded, which is degraded in a gray scale according to the time, where the black corresponds to the

https://doi.org/10.1017/S0263574717000169 Published online by Cambridge University Press

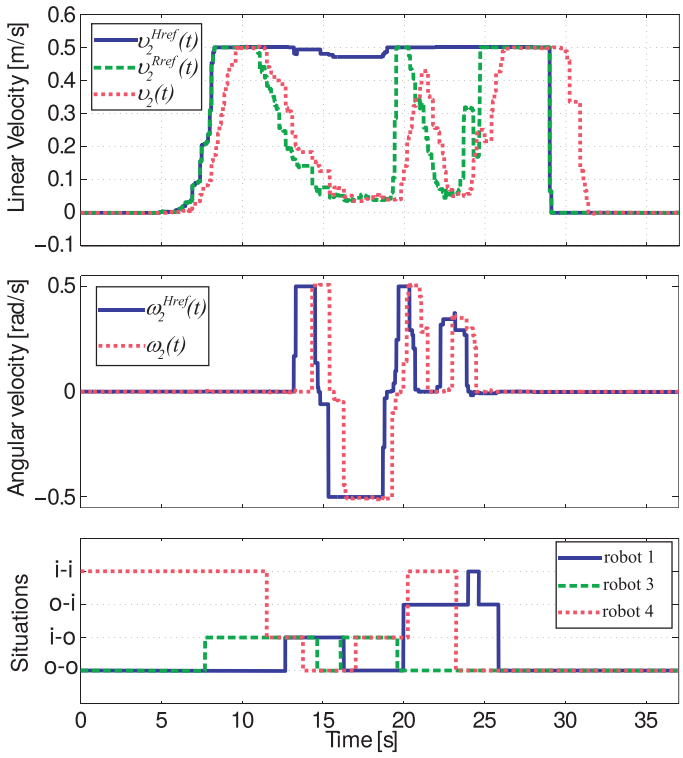


Fig. 10. User's speed reference, speed that avoid collision and current speed. Angular velocity command and current robot's angular velocity. Situations of the robot with respect to the other robots.

initial time (0 s) and white corresponds to the final time of the test. Figure 12 shows that the different positions were taken robots over time through a sequence of images.

7.2. Second test

In this test, a cross between two robots (Pioneer 3DX and Pioneer 2) teleoperated by two operators is considered. Both operators used Novint Falcon 3D joysticks. Figure 13 shows the operator 1 (left) and the operator 2 (right).

It is important to remark that the operators have visual obstruction, so each one cannot view the other robot. This causes a high probability of collision; therefore, this collision avoidance method is very useful.

In this task, only out–out situation is present; therefore, only one robot will decrease its speed to avoid collision.

Figure 14 shows the speed reference, the speed reference applied to the robots that avoid collisions and the current speed of the robots 1. In this case, only the speed command of the operator 1 is modified to avoid a collision. This is because at the time instant at which the relative velocity vector entry into the set $VO^{\tau}_{i|j}$, the speed of the robot 1 was greater than the speed of the robot 2.

Finally, the trajectories performed by the robots and an image sequence of the environment with the robots are shown in Figs. 15 and 16, respectively.

8. Discussion

In this work, tests including four mobile robots each driven by a human operator were carried out. In this case, it is possible to use small values of ρ as the number of robots is low, which is common, in practice. It is important to remark that the solution is achieved in few iterations and therefore ρ should be chosen as smaller as possible. That is, by increasing ρ a free-collision solution will be obtained, but the robots' speeds will decrease more than necessary.

https://doi.org/10.1017/S0263574717000169 Published online by Cambridge University Press

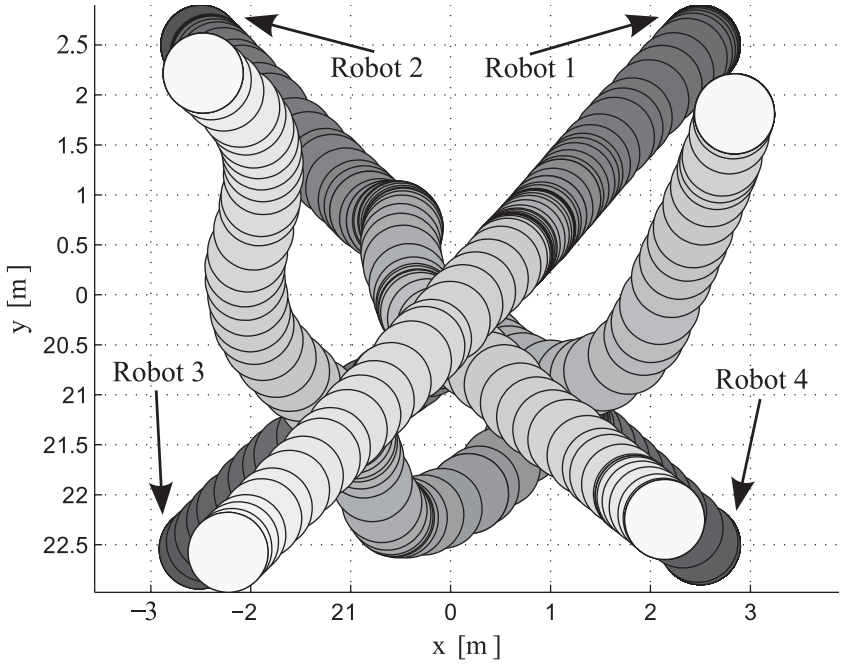


Fig. 11. Trajectories of the robots (First test).



Fig. 12. Image sequence of remote site (First Test).



Fig. 13. Operators (top) and environment with robots (Second Test).

https://doi.org/10.1017/S0263574717000169 Published online by Cambridge University Press

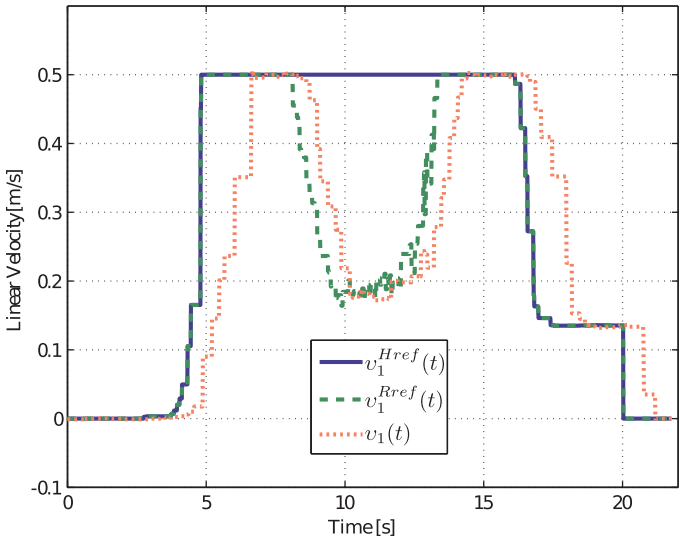


Fig. 14. Users speed, speed that avoid collision and current speed of the robot 1 (Second Test).

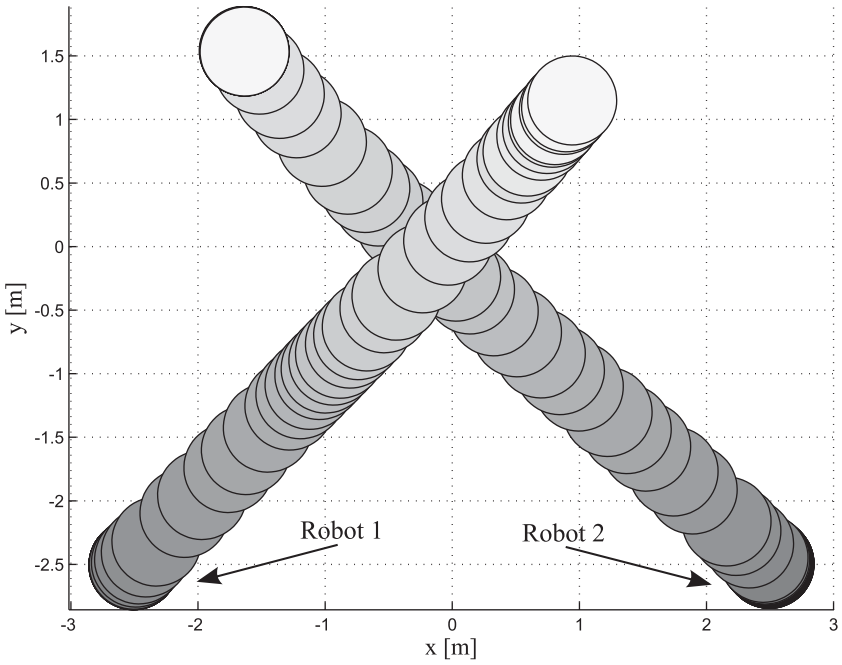


Fig. 15. Trajectories of the robots (Second test).

On the other hand, the laboratory robot speed is low. Therefore, the changes of the parameters τ and r_i do not modify significantly the behavior of the control system. In case of high velocities, the dynamic effects are relevant, and then τ and r_i should be higher.

In addition, for high-speed robots applications, an adaptable law could be proposed for adjust online τ and r_i. Another solution could involve a new method including velocity and acceleration.

When there is time delay caused by the communication channel, the method helps the operator since it acts on the remote site avoiding a possible collision. However, the stability of the delayed teleoperation system should be analyzed careful. It would be interesting to propose a stable control algorithm with force feedback that works with the SCA method.

On the other hand, the proposed method could be used in autonomous robot. In general, a path planning generating trajectories and a controller for the linear and angular velocities should be added,

https://doi.org/10.1017/S0263574717000169 Published online by Cambridge University Press

Table I. Comparisons between methods like the ORCA/NH-ORCA and SCA method.

	Methods like ORCA/NH-ORCA	SCA method
Modification of linear velocity	yes	yes
Modification of angular velocity	yes	no
Control of autonomous robot	yes	An additional algorithm would be necessary which controls the angular velocity
It always has a feasible solution	no	yes
It has a finite quantity of iterations	no	yes
Transparency in teleoperation	low	high

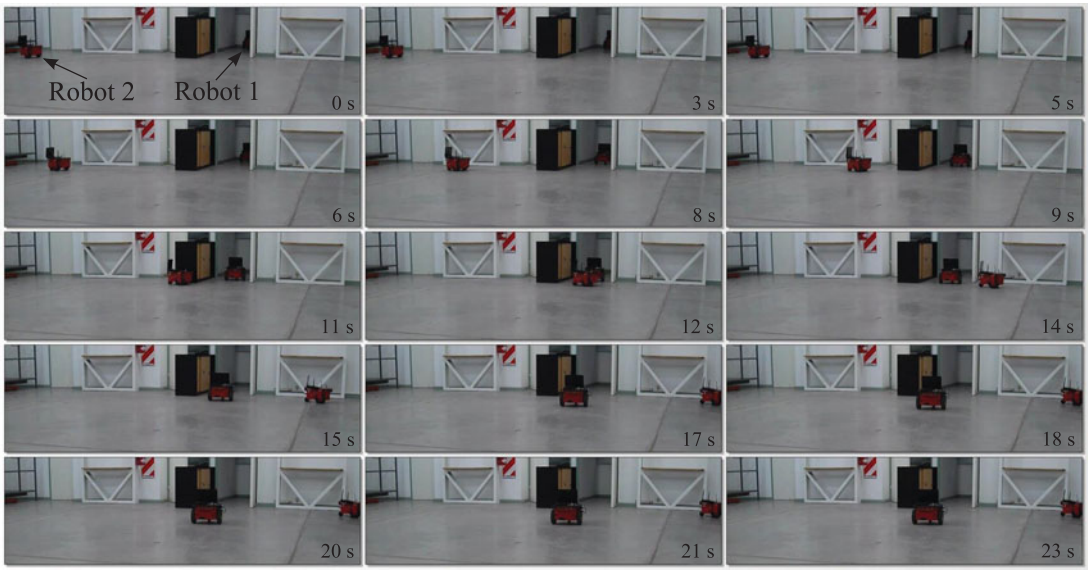


Fig. 16. Image sequence of remote site (Second Test).

and then the speed will be modified by the SCA algorithm in order to avoid collisions. Also methods like ORCA and NH-ORCA could be applied in teleoperation, but its transparency level is low. In addition, the SCA method always gets the solution, in a finite quantity of iterations. Instead, the ORCA and NH-ORCA use optimization methods and its solution could be infeasible. Also, in these methods, it is not possible to obtain a solution in a finite quantity of iterations. Table I shows a comparison between these methods.

9. Conclusion

In this paper, a method of collision avoidance for a teleoperation system with multiple human operators was proposed.

The performed analysis ensures that always one solution can be found, which is a trade-off between a fast convergence speed (less quantity of iterations) and a solution closer to the optimal (smaller change of the current velocity). It is important to point out that each iteration of the algorithm is carried out with an explicit method that does not use optimization.

Besides, experimental tests were used to verify that the design guidelines are fulfilled in practice. On the other hand, because only the reference speed is modified, the method could be applied to any kind of non-holonomic or holonomic robot moving in $\mathbb{R}^2$.

Supplementary materials

For supplementary material for this article, please visit https://doi.10.1017/S0263574717000169

https://doi.org/10.1017/S0263574717000169 Published online by Cambridge University Press

References

1. E. Slawiski, V. Mut, L. Salinas and S. García, "Teleoperation of a mobile robot with time-varying delay and force feedback," *Robotica* **30**(1), 67–77, (2012).
2. E. Slawiñski, et al. "PD-like controller with impedance for delayed bilateral teleoperation of mobile robots." *Robotica* **34**(9), 2151–2161, (2016).
3. F. Penizzotto, S. García, E. Slawiñski and V. Mut, "Delayed bilateral teleoperation of wheeled robots including a command metric," *Math. Probl. Eng.* **2015**, pp. 13, (2015).
4. S. Lichiardopol, "A survey on teleoperation," *Dept. Mech. Eng., Dynamics Control Group, Technische Universiteit Eindhoven, Eindhoven, Dept., Mech. Eng., Dyn. Control Group, The Netherlands, Tech. Rep. DCT2007*, 155 (2007).
5. T. Fong, C. Thorpe and C. Baur, "Multi-robot remote driving with collaborative control," *IEEE Trans. Ind. Electron.* **50**(4), 699–704 (2003).
6. T. Suzuki, T. Sekine, T. Fujii, H. Asama and I. Endo, "Cooperative Formation Among Multiple Mobile Robot Teleoperation in Inspection Task," *Proceedings of the 39th IEEE Conference on Decision and Control*, vol. 1 (2000) pp. 358–363.
7. D. Lee and M. W. Spong, "Bilateral Teleoperation of Multiple Cooperative Robots Over Delayed Communication Networks: Theory," *Proceedings of the 2005 IEEE International Conference on Robotics and Automation, ICRA* (2005) pp. 360–365.
8. D. Lee, O. Martinez-Palafox and M. W. Spong, "Bilateral Teleoperation of Multiple Cooperative Robots Over Delayed Communication Networks: Application," *Proceedings of the 2005 IEEE International Conference on Robotics and Automation, ICRA* (2005) pp. 366–371.
9. E. J. Rodríguez-Seda, J. J. Troy, C. A. Erignac, P. Murray, D. M. Stipanovic and M. W. Spong, "Bilateral teleoperation of multiple mobile agents: Coordinated motion and collision avoidance," *IEEE Trans. Control Syst. Technol.* **18**(4), 984–992 (2010).
10. K. Ohba, S. Kawabata, N. Y. Chong, K. Komoriya, T. Matsumaru, N. Matsuhira, K. Takase and K. Tanie, "Remote Collaboration through Time Delay in Multiple Teleoperation," *Proceedings IEEE/RSJ International Conference on Intelligent Robots and Systems, IROS' 99*, vol. 3 (1999) pp. 1866–1871.
11. N. Young Chong, T. Kotoku, K. Ohba, K. Komoriya, N. Matsuhira and K. Tanie, "Remote Coordinated Controls in Multiple Telerobot Cooperation," *Proceedings of the IEEE International Conference on Robotics and Automation, ICRA'00*, vol. 4 (2000) pp. 3138–3143.
12. N. Young Chong, S. Kawabata, K. Ohba, T. Kotoku, K. Komoriya, K. Takase and K. Tanie, "Multioperator teleoperation of multirobot systems with time delay: Part i. Aids for collision-free control," *Presence: Teleoperators Virtual Environ.* **11**(3), 277–291 (2002).
13. N. Young Chong, T. Kotoku, K. Ohba, H. Sasaki, K. Komoriya and K. Tanie, "Multioperator teleoperation of multirobot systems with time delay: Part ii. Testbed description," *Presence: Teleoperators Virtual Environ.* **11**(3), 292–303 (2002).
14. I. Elhaji, J. Tan, N. Xi, W. K. Fung, Y. H. Liu, T. Kaga, Y. Hasegawa and T. Fukuda, "Multi-Site Internet-Based Cooperative Control of Robotic Operations," *Proceedings of 2000 IEEE/RSJ International Conference on Intelligent Robots and Systems, 2000.(IROS 2000)*, vol. 2 (2000) pp. 826–831.
15. I. Elhaji, N. Xi, W. K. Fung, Y. H. Liu, Y. Hasegawa and T. Fukuda, "Modeling and Control of Internet Based Cooperative Teleoperation," *Proceedings of the IEEE International Conference on Robotics and Automation, ICRA*, vol. 1 (2001) pp. 662–667.
16. L. Wang-tai, L. Yunhui, I. H. Elhajj, N. Xi, Y. Wang and T. Fukuda, "Cooperative teleoperation of a multirobot system with force reflection via internet," *IEEE/ASME Trans. Mechatron.* **9**(4), 661–670 (2004).
17. S. Sirouspour and P. Setoodeh, "Multi-Operator/Multi-Robot Teleoperation: An Adaptive Nonlinear Control Approach," *Proceedings of the IEEE/RSJ International Conference on Intelligent Robots and Systems (IROS 2005)* (2005) pp. 1576–1581.
18. C. Passenberg, A. Peer and M. Buss, "Model-Mediated Teleoperation for Multi-Operator Multi-Robot Systems," *Proceedings of the IEEE/RSJ International Conference on Intelligent Robots and Systems (IROS)* (2010) pp. 4263–4268.
19. J. Van den Berg, S. J. Guy, M. C. Lin and D. Manocha, "Reciprocal n-Body Collision Avoidance," *Proceedings of the International Symposium on Robotics Research* (2009).
20. J. Alonso-Mora, A. Breitenmoser, M. Rufli, P. Beardsley and R. Siegwart, "Optimal Reciprocal Collision Avoidance for Multiple Non-Holonomic Robots," *Proceedings of the 10th International Symposium on Distributed Autonomous Robotic Systems (DARS)*, Berlin, Springer Press (Nov. 2010).
21. E. Slawinski and V. Mut, "Transparency in Time for Teleoperation Systems," *Proceedings of the IEEE International Conference on Robotics and Automation, ICRA* (2008) pp. 200–205.
22. E. Slawinski, V. A. Mut, P. Fiorini and L. R. Salinas, "Quantitative absolute transparency for bilateral teleoperation of mobile robots," *IEEE Trans. Syst. Man Cybern. Part A: Syst. Hum.* **42**(2), 430–442 (2012).
23. D. Bareiss and J. van den Berg, "Reciprocal Collision Avoidance for Robots with Linear Dynamics using LQR-Obstacles," *Proceedings of the IEEE International Conference Robotics and Automation* (2013).
24. P. Conroy, D. Bareiss, M. Beall and J. van den Berg, "3-D Reciprocal Collision Avoidance on Physical Quadrotor Helicopters with On-Board Sensing for Relative Positioning," *Proceedings of the IEEE/RSJ International Conference on Intelligent Robots and Systems, (IROS 2013),* (2013).
25. X. Yang, L. M. Alvarez and T. Bruggemann, "A 3D collision avoidance strategy for UAVs in a non-cooperative environment," *J. Intell. Robot. Syst.* **70**(1-4), 315–327 (2013).

https://doi.org/10.1017/S0263574717000169 Published online by Cambridge University Press

26. P. Fiorini and Z. Shiller, "Motion planning in dynamic environments using velocity obstacles," *Int. J. Robot. Res.* **17**(7), 760–772 (1998).

Appendix A. Proofs of Lemma 1 and Lemma 2

Lemma 1. *If* $\mathbf{v}_\beta \notin VO^\tau_{i|j}$ *and* $\mathbf{v}_\alpha \in \mathbb{R}^2$, *then there are values of* $\lambda > 0$ *such that* $\lambda\mathbf{v}_\alpha + \mathbf{v}_\beta \notin VO^\tau_{i|j}$.

Proof.

(1) $\mathbf{v}_\beta \notin VO^\tau_{i|j}$, and then $\mathbf{v}_\beta \in CA^\tau_{i|j}$.
(2) For definition $CA^\tau_{i|j}$ is an open set, for all $\mathbf{v}_0 \in CA^\tau_{i|j}$ there is $\epsilon \geq 0$ such that $B(\mathbf{v}_0, \epsilon) \subset CA^\tau_{i|j}$ where $B(\mathbf{v}_0, \epsilon) = \{\mathbf{v} \in \mathbb{R}^2 \mid \|\mathbf{v} - \mathbf{v}_0\| \leq \epsilon\}$.
(3) Taking in $\{2\}$ $\mathbf{v}_0 = \mathbf{v}_\beta$ and choosing $\mathbf{v} = \lambda\mathbf{v}_\alpha + \mathbf{v}_\beta$, it is simple to deduce that

$$-\frac{\epsilon}{\|\mathbf{v}_\alpha\|} < \lambda < \frac{\epsilon}{\|\mathbf{v}_\alpha\|}$$

Therefore, there are values of $\lambda \geq 0$ such that $\lambda\mathbf{v}_\alpha + \mathbf{v}_\beta \in B(\mathbf{v}_\beta, \epsilon)$, and consequently $\lambda\mathbf{v}_\alpha + \mathbf{v}_\beta \in CA^\tau_{i|j}$; therefore, $\lambda\mathbf{v}_\alpha + \mathbf{v}_\beta \notin VO^\tau_{i|j}$. The proof is complete. □

Lemma 2. *If* $\mathbf{v}_i \in VO^\infty_{i|j}$ *and* $-\mathbf{v}_j \in VO^\infty_{i|j}$, *then* $\lambda_i\mathbf{v}_i - \lambda_j\mathbf{v}_j \in VO^\infty_{i|j}$ *for* $\lambda_i > 0$ *and* $\lambda_j > 0$.

Proof.

(1) $2\lambda_i t \in [0, \infty)$ and $2\lambda_j t \in [0, \infty)$ due to $t \in [0, \infty)$.
(2) Replacing $2\lambda_i t$ and $2\lambda_j t$ for t in (2), the following inequalities are obtained:

$$\|2\lambda_i t\mathbf{v}_i - (\mathbf{p}_j - \mathbf{p}_i)\| \leq r_i + r_j \text{ and } \|-2\lambda_j t\mathbf{v}_j - (\mathbf{p}_j - \mathbf{p}_i)\| \leq r_i + r_j$$

(3) From $\{2\}$ and applying the triangle inequality:

$$r_i + r_j \geq \left\|\frac{2\lambda_i t\mathbf{v}_i - (\mathbf{p}_j - \mathbf{p}_i)}{2}\right\| + \left\|\frac{-2\lambda_j t\mathbf{v}_j - (\mathbf{p}_j - \mathbf{p}_i)}{2}\right\| \geq \left\|t\left(\lambda_i\mathbf{v}_i - \lambda_j\mathbf{v}_j\right) - (\mathbf{p}_j - \mathbf{p}_i)\right\|$$

Then, $t(\lambda_i\mathbf{v}_i - \lambda_j\mathbf{v}_j) \in B(\mathbf{p}_j - \mathbf{p}_i, r_i + r_j)$, and therefore, $(\lambda_i\mathbf{v}_i - \lambda_j\mathbf{v}_j) \in VO^\infty_{i|j}$. The proof is complete. □

Appendix B. Obtaining of the Vectors $\mathbf{q}_1$ and $\mathbf{q}_2$, and the Upper Bounds λ_{i_1}, λ_{i_2} and λ_{i_3} from Section 4.1

Vectors $\mathbf{q}_1$ and $\mathbf{q}_2$ can be expressed in terms of the vectors $\mathbf{h}_1$ and $\mathbf{h}_2$, respectively (see Fig. 4) as follows:

$$\mathbf{q}_l = \frac{\mathbf{p}_j - \mathbf{p}_i}{\tau} + \frac{r_i + r_j}{\tau}\mathbf{h}_l \quad \text{for } l = 1, 2 \text{ and } \|\mathbf{h}_l\| = 1 \tag{A1}$$

In addition, $\mathbf{q}_l$ is orthogonal to $\mathbf{h}_l$ for $l = 1, 2$; therefore:

$$\mathbf{q}_l^T\mathbf{h}_l = 0 \quad \text{for } l = 1, 2 \tag{A2}$$

Replacing (A1) in (A2), the following equation is obtained:

$$\left(\frac{\mathbf{p}_j - \mathbf{p}_i}{\tau} + \frac{r_i + r_j}{\tau}\mathbf{h}_l\right)^T \mathbf{h}_l = 0 \quad \text{for } l = 1, 2 \tag{A3}$$

https://doi.org/10.1017/S0263574717000169 Published online by Cambridge University Press

Applying distributive property and multiplying by τ, we get:

$$\left(\mathbf{p}_j - \mathbf{p}_i\right)^T \mathbf{h}_l + \left(r_i + r_j\right) \|\mathbf{h}_l\| = 0 \quad \text{for } l = 1, 2 \tag{A4}$$

As $\|\mathbf{h}_l\| = 1$, Eq. (A4) gives as results the following equations system:

$$\left(p_{j_x} - p_{i_x}\right) h_{l_x} + \left(p_{j_y} - p_{i_y}\right) h_{l_y} + \left(r_i + r_j\right) = 0 \tag{A5a}$$

$$h_{l_x}^2 + h_{l_y}^2 = 1 \tag{A5b}$$

where $\mathbf{p}_i = [p_{i_x} \;\; p_{i_y}]^T$, $\mathbf{p}_j = [p_{j_x} \;\; p_{j_y}]^T$ and $\mathbf{h}_l = [h_{l_x} \;\; h_{l_y}]^T$. By operating, the following solution of (A5a) and (A5b) is obtained:

$$h_{1_x} = \frac{-(r_i + r_j)\left(p_{j_x} - p_{i_x}\right) - \mu\left(p_{j_y} - p_{i_y}\right)}{\left\|\mathbf{p}_j - \mathbf{p}_i\right\|^2} \tag{A6a}$$

$$h_{1_y} = \frac{-(r_i + r_j)\left(p_{j_y} - p_{i_y}\right) + \mu\left(p_{j_x} - p_{i_x}\right)}{\left\|\mathbf{p}_j - \mathbf{p}_i\right\|^2} \tag{A6b}$$

$$h_{2_x} = \frac{-(r_i + r_j)\left(p_{j_x} - p_{i_x}\right) + \mu\left(p_{j_y} - p_{i_y}\right)}{\left\|\mathbf{p}_j - \mathbf{p}_i\right\|^2} \tag{A6c}$$

$$h_{2_y} = \frac{-(r_i + r_j)\left(p_{j_y} - p_{i_y}\right) - \mu\left(p_{j_x} - p_{i_x}\right)}{\left\|\mathbf{p}_j - \mathbf{p}_i\right\|^2} \tag{A6d}$$

where $\mu = \sqrt{\|\mathbf{p}_j - \mathbf{p}_i\|^2 - (r_i + r_j)^2}$.

These equations can be expressed in matrix form by

$$\mathbf{h}_1 = \left(\frac{-(r_i + r_j)\mathbf{I} + \mu\mathbf{R}}{\left\|\mathbf{p}_j - \mathbf{p}_i\right\|^2}\right)\left(\mathbf{p}_j - \mathbf{p}_i\right) \tag{A7a}$$

$$\mathbf{h}_2 = \left(\frac{-(r_i + r_j)\mathbf{I} - \mu\mathbf{R}}{\left\|\mathbf{p}_j - \mathbf{p}_i\right\|^2}\right)\left(\mathbf{p}_j - \mathbf{p}_i\right) \tag{A7b}$$

where $\mathbf{R} = \left[\begin{smallmatrix} 0 & -1 \\ 1 & 0 \end{smallmatrix}\right]$. Then, replacing (A7a) and (A7b) in (A1), $\mathbf{q}_1$ and $\mathbf{q}_2$ are obtained (the resulting equations are (8a) and (8b)).

On the other hand, the upper bounds λ_{i_1} and λ_{i_2} from Section 4.1 are obtained as follows:

The intersection between (6) and (7) results:

$$\lambda_{i_l}\mathbf{v}_i - \mathbf{v}_j = \gamma_l \mathbf{q}_l \quad \text{for } l = 1, 2 \tag{A8}$$

Equation (A8) can be expressed by the following equations system:

$$\lambda_{i_l} v_{i_x} - v_{j_x} = \gamma_l q_{l_x} \tag{A9a}$$

$$\lambda_{i_l} v_{i_y} - v_{j_y} = \gamma_l q_{l_y} \tag{A9b}$$

where $\mathbf{v}_i = [v_{i_x} \;\; v_{i_y}]^T$, $\mathbf{v}_j = [v_{j_x} \;\; v_{j_y}]^T$ and $\mathbf{q}_l = [q_{l_x} \;\; q_{l_y}]^T$.

Operating (A9a) and (A9b), it is possible to obtain:

$$\lambda_{i_l} = \frac{v_{j_x} q_{l_y} - v_{j_y} q_{l_x}}{v_{i_x} q_{l_y} - v_{i_y} q_{l_x}} \quad \text{for } l = 1, 2 \tag{A10a}$$

https://doi.org/10.1017/S0263574717000169 Published online by Cambridge University Press

$$\gamma_l = \frac{v_{j_x} v_{i_y} - v_{j_y} v_{i_x}}{v_{i_x} q_{l_y} - v_{i_y} q_{l_x}} \quad \text{for } l = 1, 2 \tag{A10b}$$

Equations (A10a) and (A10b) can be written in matrix form like (11a) and (11b).

Finally, the upper bound λ_{i_3} of subsection 4.1 is obtained as follows:
The intersection between (6) and (9) results

$$\lambda_{i_3} \mathbf{v}_i - \mathbf{v}_j = \frac{\mathbf{p}_j - \mathbf{p}_i}{\tau} + \frac{r_i + r_j}{\tau} [\cos(\theta) \quad \sin(\theta)]^T \tag{A11}$$

Equation (A11) can be expressed by the following equations system:

$$\lambda_{i_3} v_{i_x} - v_{j_x} - \frac{p_{j_x} - p_{i_x}}{\tau} = \frac{r_i + r_j}{\tau} \cos(\theta) \tag{A12a}$$

$$\lambda_{i_3} v_{i_y} - v_{j_y} - \frac{p_{j_y} - p_{i_y}}{\tau} = \frac{r_i + r_j}{\tau} \sin(\theta) \tag{A12b}$$

Dividing (A12b) by (A12a) and solving for θ, we get:

$$\theta = \arctan\left(\frac{\lambda_{i_3} v_{i_y} - v_{j_y} - \frac{p_{j_y} - p_{i_y}}{\tau}}{\lambda_{i_3} v_{i_x} - v_{j_x} - \frac{p_{j_x} - p_{i_x}}{\tau}} \right) \tag{A13}$$

Replacing (A13) in (A12b):

$$\lambda_{i_3} v_{i_y} - v_{j_y} - \frac{p_{j_y} - p_{i_y}}{\tau} = \frac{r_i + r_j}{\tau} \sin\left(\arctan\left(\frac{\lambda_{i_3} v_{i_y} - v_{j_y} - \frac{p_{j_y} - p_{i_y}}{\tau}}{\lambda_{i_3} v_{i_x} - v_{j_x} - \frac{p_{j_x} - p_{i_x}}{\tau}} \right) \right) \tag{A14}$$

Using the relation $\sin(\arctan(x)) = x/\sqrt{1 + x^2}$ in (A14) and by solving it, the next quadratic polynomial is obtained:

$$\begin{aligned} &\left(v_{i_x}^2 + v_{i_y}^2\right) \lambda_{i_3}^2 - 2 \left(v_{i_x} \left(v_{j_x} + \frac{p_{j_x} - p_{i_x}}{\tau} \right) + v_{i_y} \left(v_{j_y} + \frac{p_{j_y} - p_{i_y}}{\tau} \right) \right) \lambda_{i_3} \\ &+ \left(v_{j_x} + \frac{p_{j_x} - p_{i_x}}{\tau} \right)^2 + \left(v_{j_y} + \frac{p_{j_y} - p_{i_y}}{\tau} \right)^2 = 0 \end{aligned} \tag{A15}$$

$$\begin{aligned} \lambda_{i_3} = &\frac{v_{i_x} \left(\frac{p_{j_x} - p_{i_x}}{\tau} + v_{j_x} \right) + v_{i_y} \left(\frac{p_{j_y} - p_{i_y}}{\tau} + v_{j_y} \right)}{\|\mathbf{v}_i\|^2} \\ &- \frac{\sqrt{\|\mathbf{v}_i\|^2 \left(\frac{r_i + r_j}{\tau} \right)^2 - \left(v_{i_x} \left(\frac{p_{j_y} - p_{i_y}}{\tau} + v_{j_y} \right) - v_{i_y} \left(\frac{p_{j_x} - p_{i_x}}{\tau} + v_{j_x} \right) \right)^2}}{\|\mathbf{v}_i\|^2} \end{aligned} \tag{A16}$$

Then, the solution that corresponds to the intersections between $\mathbf{v}_{i|j}(\lambda_i)$ (Eq. (6)) and the $\mathbf{arc}(\theta)$ (Eq. (9)) is given by Eq. (A16), which can be expressed in matrix form like (12).

https://doi.org/10.1017/S0263574717000169 Published online by Cambridge University Press